Radiative lifetime measurements in TmIII with time-resolved laser spectroscopy and comparisons with HFR calculations

Li, Z. S; Zhang, Z. G; Lokhnygin, V; Svanberg, Sune; Bastin, T; Biemont, E; Garnir, H. P; Palmeri, P; Quinet, P

Published in:
Journal of Physics B: Atomic, Molecular and Optical Physics

DOI:
10.1088/0953-4075/34/8/301

2001

Radiative lifetime measurements in Tm III with time-resolved laser spectroscopy and comparisons with HFR calculations

2001 J. Phys. B: At. Mol. Opt. Phys. 34 1349

(http://iopscience.iop.org/0953-4075/34/8/301)

INSTITUTE OF PHYSICS PUBLISHING JOURNAL OF PHYSICS B: ATOMIC, MOLECULAR AND OPTICAL PHYSICS

J. Phys. B: At. Mol. Opt. Phys. **34** (2001) 1349–1359 www.iop.org/Journals/jb PII: S0953-4075(01)15375-7

Radiative lifetime measurements in Tm III with time-resolved laser spectroscopy and comparisons with HFR calculations

Z S Li[1], Z G Zhang[1], V Lokhnygin[1], S Svanberg[1], T Bastin[2], E Biémont[2,3], H P Garnir[2], P Palmeri[3] and P Quinet[2,3]

[1] Department of Physics, Lund Institute of Technology, PO Box 118, S-221 00 Lund, Sweden
[2] Institut de Physique Nucléaire Expérimentale (Bât. B 15), Université de Liège, B-4000 Liège, Belgium
[3] Astrophysique et Spectroscopie, Université de Mons-Hainaut, B-7000 Mons, Belgium

Received 10 July 2000, in final form 21 February 2001

Abstract

Natural radiative lifetimes of eight levels in Tm III were measured with the time-resolved laser-induced fluorescence (LIF) technique. Free doubly ionized thulium ions were obtained in a laser-produced plasma. Three even-parity levels were excited from the ground state with one-photon excitation, using a laser system generating pulses of 1 ns duration. Five odd-parity levels were excited from the ground state with two-photon excitation, where a picosecond laser system was employed. In both cases, the lifetimes were evaluated from transient LIF signals detected with a fast-detection system. The experimental lifetime results were compared with Hartree–Fock calculations including relativistic corrections. Good agreement was achieved for the $4f^{12}6p$ levels while larger discrepancies are noted for some $4f^{12}5d$ levels.

(Some figures in this article are in colour only in the electronic version; see `www.iop.org`)

1. Introduction

The lanthanide elements are important in astrophysics in relation to nucleosynthesis and star formation considerations. Investigations of the third spectrum of rare-earth elements are motivated by the astrophysical interest because, in the hot chemically peculiar stars, the doubly ionized ions are typically the dominant ionization stage. This has stimulated a few studies of the third spectrum of rare-earth elements, such as Dy III (Spector *et al* 1997), Er III (Wyart *et al* 1997), Ce III (Bord *et al* 1997, Wyart and Palmeri 1998) and Nd III (Cowley and Bord 1998). However, the oscillator strength data, which are needed for the quantitative analysis of stellar spectra, are scarcely available.

The most reliable method of determining the oscillator strengths is the combination of experimental lifetime values with branching fractions. The recently published lifetime measurements on La III by Li and Jiang (1999) are believed to constitute the first lifetime results of doubly ionized lanthanide ions using selective laser excitation and a cascade-free detection

method. Following that, laser spectroscopic lifetime measurements on Eu III (Zhang *et al* 2000), Lu III (Wahlgren *et al* 2001, Fedchak *et al* 2000), Ce III (Li *et al* 2000) and Er III (Biémont *et al* 2001) were also performed. For the joint purpose of providing data for testing theoretical calculations as well as application to astrophysics, in particular for stellar elemental abundance analyses, systematic investigations of radiative lifetimes of doubly charged lanthanide elements have been undertaken.

This paper is focused on the determination of the radiative properties of Tm III. Thulium has a single stable isotope with mass number 169 and nuclear spin $I = 1/2$. The third spectrum of thulium was first analysed by Sugar (1970). Later, Wyart *et al* (1974) gave the parameter values obtained from a calculation, which included the configuration interaction of $4f^{12}5d$ and $4f^{12}6s$. Based on the above work, Martin *et al* (1978) tabulated the energy levels. Large-scale laser spectroscopic lifetime measurements on Tm I and Tm II were published by Anderson *et al* (1996), where most of the previous lifetime results were compiled, but no experimental results of oscillator strength and radiative lifetime determination for Tm III were available prior to our work.

In our recent theoretical work, improved relativistic Hartree–Fock (HFR) calculations have been performed. Good agreement with the experimental lifetime results was achieved for Yb II (Li *et al* 1999a) and for the third spectrum of La and Lu (Biémont *et al* 1999). Confirmed by the good agreement between the experimental and theoretical radiative lifetimes, reliable oscillator strength values were derived.

In this paper, lifetimes of three even-parity and five odd-parity levels in Tm III were measured with time-resolved laser spectroscopy. A comprehensive HFR calculation with consideration of extended configuration interaction and core-polarization effects was also performed.

The Tm^{2+} ion has 67 electrons and the ground configuration is $4f^{13}$. A partial energy level diagram relevant to this experiment is shown in figure 1.

2. Experimental arrangement

2.1. Plasma production

A laser-produced plasma was utilized as the Tm^{2+} ion source. The plasma was produced by focusing, on a solid thulium target placed in a vacuum chamber, the green beam of a Continuum Surelite Nd:YAG laser. The pulse has a duration of 10 ns and an energy of $\sim$5 mJ. This plasma has proved to be a versatile source of unperturbed atoms, and singly and doubly charged ions (see, e.g., Li *et al* (2000)). All the excitations in the present experiment are from the ground state, reducing the effect of collisional quenching and relaxing the plasma temperature and density requirements. The excitation schemes adopted are shown in figure 1.

2.2. Single-photon excitation

The laser system used for the one-photon transition experiment is shown in figure 2. A Nd:YAG laser (Continuum NY-82), which was used to pump the dye laser (Continuum ND-60), has a pulse duration of 8 ns. A compressor, based on stimulated Brillouin scattering in water, was utilized to shorten the pulse duration to 1 ns. A detailed description of this system can be found in Li *et al* (1999b). The dye laser which operates on the DCM dye has a tunable region from 615 to 660 nm. A nonlinear conversion system, which includes a KDP crystal, a BBO crystal and a retarding plate, was utilized to triple the dye laser output in order to reach the required short wavelengths. The KDP crystal was used for frequency doubling; then by mixing with

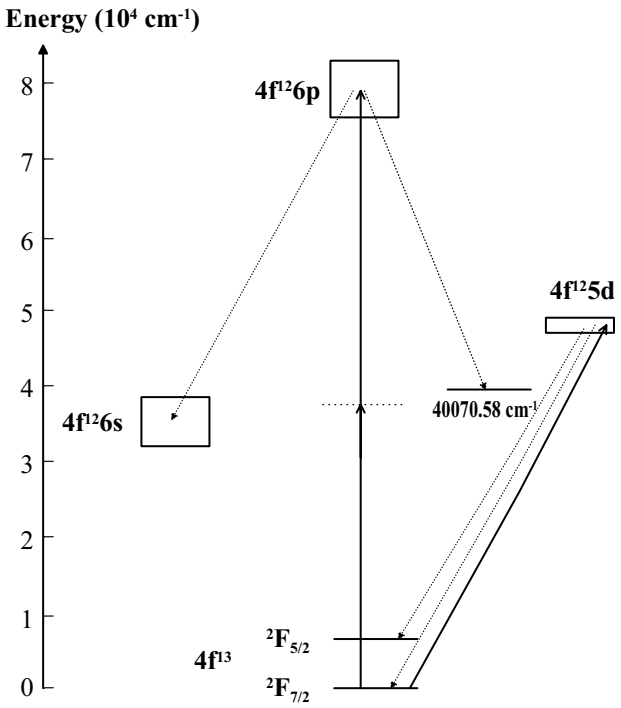

Figure 1. Partial Grotrian diagram and excitation schemes.

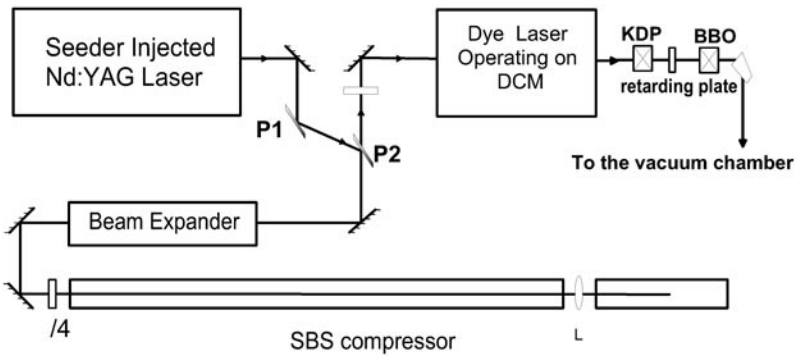

Figure 2. Nanosecond laser system.

the remaining fundamental beam in the BBO crystal, frequency tripling was achieved. The retarding plate was utilized to rotate the polarization direction of both beams to become parallel to each other. Three levels belonging to the 4f^{12}5d configuration were excited, starting from the ground configuration, by tuning the laser wavelength to the appropriate values (table 1).

2.3. Two-photon excitation

The picosecond laser system employed for two-photon excitation is shown schematically in figure 3. A *Q*-switched and mode-locked Nd:YAG laser provides 25 mJ green pulses with a duration of 70 ps (measured with a streak camera). A distributed feedback dye (DFDL) laser

Table 1. Levels measured and excitation schemes.

Excited level[a] (cm^{-1})	Excitation wavelength λ (nm)	Lower level[a] (cm^{-1})	Observed fluorescence λ (nm)
45 732.62	218.66	0	219
45 794.62	218.37	0	218
47 624.18	209.98	0/8774.03	210/270
76 721.50	2 × 260.68	40 070.58	272.8
76 807.38	2 × 260.39	33 831.91	232.7
81 011.48	2 × 246.88	38 055.53	232.8
82 440.04	2 × 242.60	39 882.62	236.0
82 573.05	2 × 242.21	39 882.62	234.2

[a] Martin *et al* (1978).

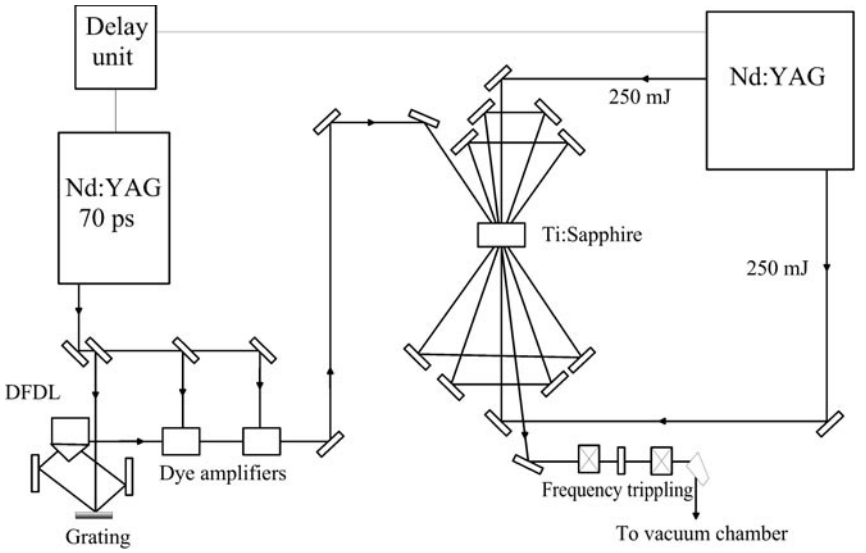

Figure 3. Picosecond laser system.

was pumped with this beam. The output from the DFDL laser was amplified by two linear dye stages and in a Ti:sapphire crystal butterfly amplifier, which were pumped by another Nd:YAG (Continuum NY-82) laser. Frequency tripling was performed in an optical crystal system, which is similar to the one described in the above paragraph, to reach the required wavelength region.

Five levels from the $4f^{12}6p$ configuration were populated from the ground state by two-photon absorption. The choice of these five levels is due to the existence of some states from the $4f^{12}5d$ configuration, which are close to the intermediate virtual level and have reasonable strong transition probabilities to both the ground and upper levels to be studied. The presence of these middle levels effectively enhances this two-photon excitation process. The excitation and observed fluorescence transition for these five levels are also indicated in table 1.

2.4. Signal observation

The setup of the whole system is shown in figure 4. All Nd:YAG lasers were working in the external triggering mode, and were activated by the same delay generator, which enables

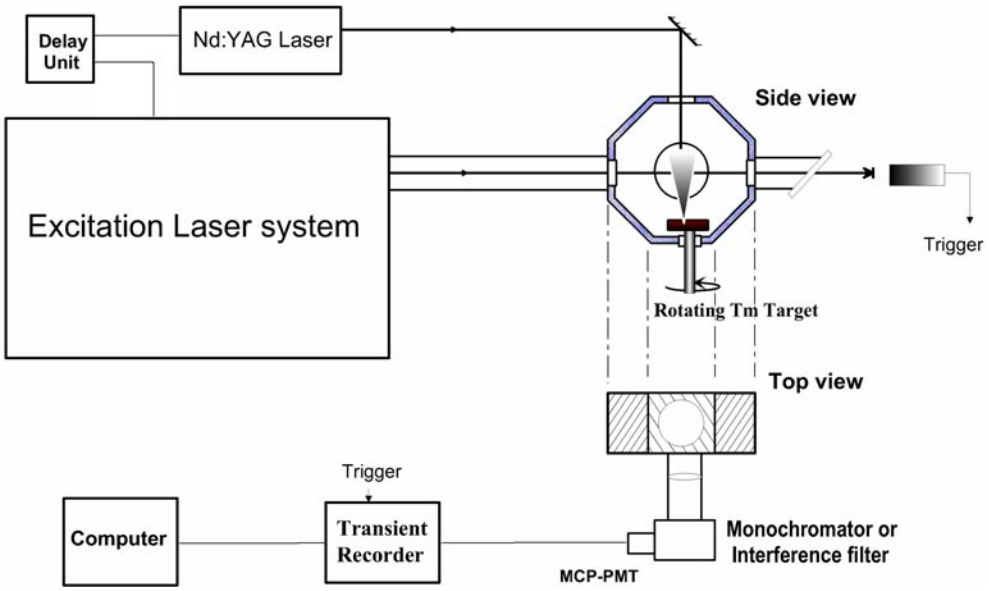

Figure 4. Experimental setup.

the temporal synchronization of the atomization and excitation pulses. Fluorescence photons were collected with a fused-silica lens, filtered by a 25 cm monochromator or an interference filter, and were finally detected by a Hamamatsu 1564U microchannel plate photomultiplier tube (200 ps rise time). The interference filter, which has a much larger acceptance area, was utilized for the long lived states to avoid 'flight-out-of-view' effects. A strong magnetic field was applied to wash out potential distortion of the decay signal by Zeeman quantum beats. The transient signals were captured by a Tektronix TDS 684B transient digitizer (1 GHz bandwidth and real time 5Gsample s^{-1}), which was triggered from a Thorlabs SV2-FC photo-diode (120 ps rise time) driven by the excitation beam.

Saturation of the detector was carefully avoided during the experiments, especially for short-lived states. Only very weak signal were detected, and an average of 1000–4000 pulses was performed to obtain smooth signals with reasonable signal-to-noise ratio.

2.5. Data analysis

The digitalized signals were transferred to a personal computer, and on-line lifetime evaluations were performed to support the measurements.

As the lifetime values of the $4f^{12}5d$ levels are much longer than 1 ns, a direct exponential fit can be performed to evaluate the lifetimes from the detected time-resolved fluorescence signals. A typical fluorescence signal is shown in figure 5 with the exponential fitting. The unfitted part in the beginning of the signal comes from the scattering light of the excitation pulse as the resonance line was chosen to record the exponential decay.

The other levels have lifetimes of the order of 2 ns, which is comparable with the time resolution of the detection system. It is thus necessary to take into account the temporal response of the system in order to analyse the decay curves. The recording of the pico-laser signal scattered by a metal rod inserted into the observation region gives the temporal response of the detection system as the pico-laser pulse width is considerably shorter than the time

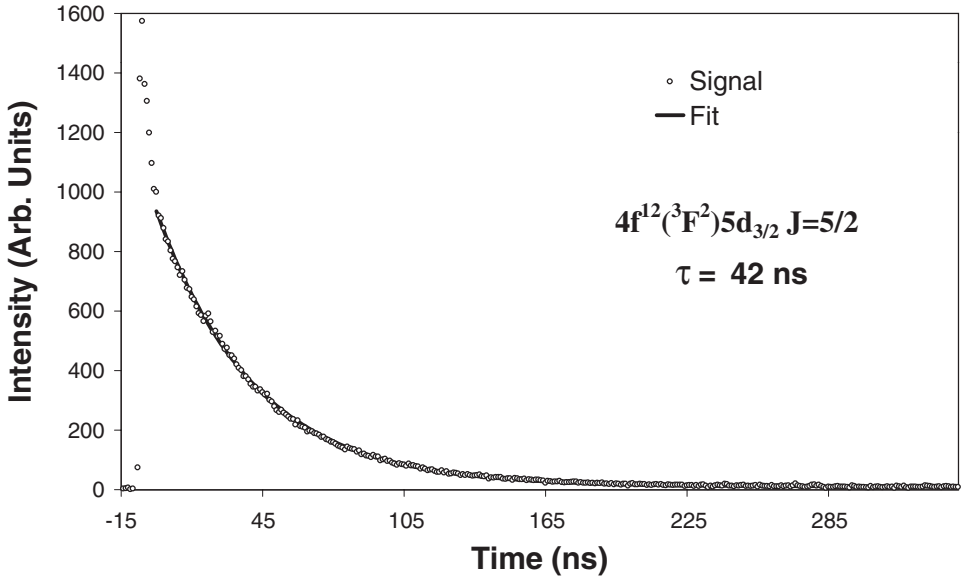

Figure 5. A typical detected fluorescence signal from a $4f^{12}5d$ level, with an exponential fitting.

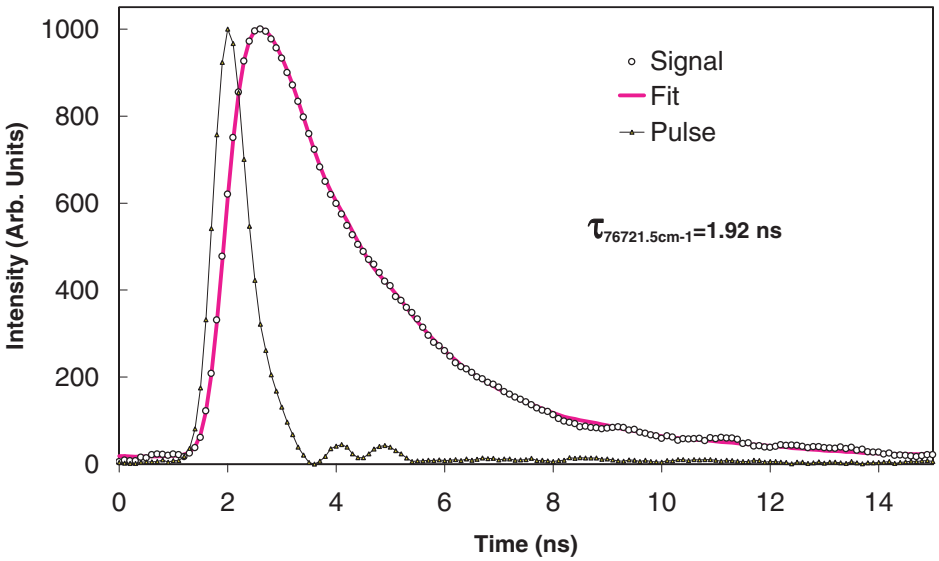

Figure 6. A typical detected fluorescence signal from a $4f^{12}6p$ level, with a convolutional fitting.

resolution of the system. By fitting to the recorded transient LIF signal the convolution of the pico-laser response curve with an exponential decay the proper lifetime information can be accurately extracted. A typical fluorescence curve with a convolutional fit is shown in figure 6.

Table 2. Experimental lifetimes and comparison with the theoretical results.

Levels		Lifetimes (ns)	
Designations[a]	Energy (cm^{-1})	Experimental	Theoretical[b]
$4f^{12}(^3H_4)5d_{3/2}$ $J = 7/2$	45 732.62	32 ± 3	21
$4f^{12}(^1G_4)5d_{5/2}$ $J = 7/2$	45 794.62	71 ± 7	67
$4f^{12}(^3F_2)5d_{3/2}$ $J = 5/2$	47 624.18	41 ± 3	30
$4f^{12}(^3F_3)6p_{1/2}(5, 1/2)^o_{5/2}$	76 721.50	1.92 ± 0.15	2.14
$4f^{12}(^3H_5)6p_{3/2}(5, 3/2)^o_{9/2}$	76 807.38	1.52 ± 0.15	1.51
$4f^{12}(^3H_4)6p_{3/2}(4, 3/2)^o_{7/2}$	81 011.48	1.45 ± 0.15	1.49
$4f^{12}(^3F_3)6p_{3/2}(3, 3/2)^o_{7/2}$	82 440.04	1.47 ± 0.15	1.50
$4f^{12}(^3F_3)6p_{3/2}(3, 3/2)^o_{5/2}$	82 573.05	1.40 ± 0.15	1.50

[a] Martin *et al* (1978).
[b] Calculation A (see the text).

3. Measurements and results

The Tm^{2+} ions were obtained in the laser-produced plasma by a proper choice of the plasma parameters. This was achieved by varying the ablation laser pulse energy, the focus size, the height of the excitation beam above the ablation point and the delay time between the atomization and excitation pulses. As the plasma was hotter when preparing the doubly ionized ions, the investigation of collisional effects is important especially for the 5d levels which have relatively longer lifetimes. When varying the delay time between the ablation and excitation laser pulses from 1 to 1.5 μs, the detected fluorescence intensity can change by a factor of almost 15 from 3 to 40 mV, which reflects that the ionic density in the excitation spot has been dramatically changed. The evaluated lifetimes from those signals remain constant within the statistical scattering. This confirmed that the collisional effects as well as the radiation trapping effects were negligible under the present experimental conditions.

The results are shown in table 2, where the quoted error bars reflect not only the statistical scattering, but also a conservative estimate (10%) of the possible remaining systematic errors such as residual collisional effects. The level assignments and energies in the table are from Martin *et al* (1978).

4. HFR calculations

The theoretical method considered in this paper is the HFR technique developed by Cowan (1981) in which we have included the core-polarization and core-penetration effects (see, for example, Biémont *et al* (1998, 1999), Quinet *et al* (1999a, b)). For the configurations of the type $4f^{12}nl$, we have used the value of the static dipole polarizability of Tm IV computed by Fraga *et al* (1976): $\alpha_d = 5.60\ a_0^3$. The cut-off radius, r_c, has been chosen equal to $1.42\ a_0$: this corresponds to the HFR average value $\langle r \rangle$ for the outermost core orbitals ($5p^6$) of the investigated configurations. With 4f electrons deeply embedded inside the closed $5s^25p^6$ subshells, the analytical core-polarization corrections to the dipole operator as introduced in our model (see equation (6) in Quinet *et al* (1999b)) are no longer valid for transitions involving these electrons. Instead, we have applied a scaling factor to the uncorrected $\langle 4f|r|5d \rangle$ radial matrix element corresponding to the $4f^{13}$–$4f^{12}5d$ transition array according to the procedure already used in the case of Er III (Biémont *et al* 2000). This is illustrated in figure 7, in which we have reported the ratio between core-polarization corrected (d_{pol}) and uncorrected

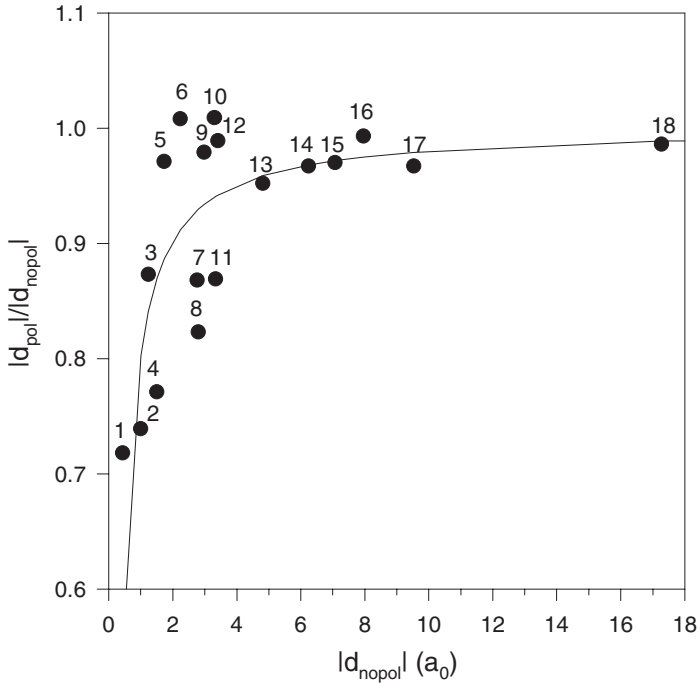

Figure 7. Absolute value of the ratio between transition matrix elements corrected by core-polarization effects ($d_{\rm pol}$) and uncorrected matrix elements ($d_{\rm nopol}$) of transitions not involving a 4f electron as a function of the absolute value of the uncorrected data. The meaning of the symbols is as follows ($4f^{12}$ being the core): 1: 5d–7p; 2: 5d–7f; 3: 6p–7d; 4: 5d–6f; 5: 6d–7f; 6: 6p–7s; 7: 5d–6p; 8: 5d–5f; 9: 6d–6f; 10: 5f–7d; 11: 6s–6p; 12: 7d–7f; 13: 6p–6d; 14: 7s–7p; 15: 6d–7p; 16: 7p–7d; 17: 5f–6d; 18: 6f–7d.

($d_{\rm nopol}$) transition matrix elements for transitions not involving a 4f electron as a function of the uncorrected matrix element. A smooth curve was obtained by plotting $|d_{\rm nopol} - \Delta|/|d_{\rm nopol}|$, where Δ is the mean value of $|d_{\rm nopol} - d_{\rm pol}|$ for the transitions not involving a 4f electron. In order to take polarization effects into account for the 4f–5d transitions, the uncorrected $\langle 4f|r|5d\rangle$ radial matrix element (=1.079 a_0) has been scaled down by the factor 0.81 deduced from the curve of figure 7.

Valence correlation has been considered among the following configurations: $4f^{13}$ + $4f^{12}6p$ + $4f^{12}7p$ + $4f^{12}5f$ + $4f^{12}6f$ + $4f^{12}7f$ for the odd parity and $4f^{12}5d$ + $4f^{12}6d$ + $4f^{12}7d$ + $4f^{12}6s$ + $4f^{12}7s$ for the even parity (calculation A).

In our paper, the HFR method has been combined with a least-squares optimization routine minimizing the discrepancies between the calculated energy levels and the experimental values compiled by Martin *et al* (1978). The average energies ($E_{\rm av}$), the Slater parameters (F^k, G^k) and the spin–orbit integrals (ζ_{nl}) corresponding to the $4f^{13}$, $4f^{12}6p$, $4f^{12}5d$ and $4f^{12}6s$ were adjusted. The F^k, G^k and R^k integrals, not optimized in the fitting procedure, were arbitrarily scaled down by a factor 0.85 in agreement with a well-established practice (Cowan 1981). For the configurations $4f^{12}7p$, $4f^{12}5f$, $4f^{12}6f$, $4f^{12}7f$, $4f^{12}6d$, $4f^{12}7d$ and $4f^{12}7s$, the *ab initio* average energies were increased by 20 000 cm^{-1} by analogy with the fitted values obtained for $4f^{12}6p$, $4f^{12}5d$ and $4f^{12}6s$. This quite large correction to the average energies of $4f^{12}nl$ configurations might be explained by the fact that the relative differences between the calculated values of $E_{\rm av}$ ($4f^{12}nl$) and $E_{\rm av}$ ($4f^{13}$) could be inaccurate because of the extreme relaxation

Table 3. Oscillator strengths (log gf) and transition probabilities (gA) for the lines involving the $4f^{12}6p$ levels appearing in table 2. Only lines with gA-values greater than 10^8 s^{-1} are reported in the table.

Wavelength[a] (Å)	Lower level[b]		Upper level[b]					
	E (cm^{-1})	J	E (cm^{-1})	J	log gf_{HFR}[c]	gA_{HFR}[c] (s^{-1})	log gf_{norm}[d]	gA_{norm}[d] (s^{-1})
2324.429	38 003 (e)	9/2	81 011 (o)	7/2	−0.42	4.64E+08	−0.41	4.77E+08
2324.620	33 803 (e)	5.5	76 807 (o)	9/2	−0.27	6.69E+08	−0.27	6.64E+08
2326.195	33 832 (e)	9/2	76 807 (o)	9/2	0.45	3.45E+09	0.45	3.43E+09
2327.252	38 056 (e)	7/2	81 011 (o)	7/2	0.34	2.71E+09	0.35	2.79E+09
2338.441	39 823 (e)	5/2	82 573 (o)	5/2	0.14	1.66E+09	0.17	1.78E+09
2344.589	39 935 (e)	7/2	82 573 (o)	5/2	−0.98	1.27E+08	−0.95	1.36E+08
2345.740	39 823 (e)	5/2	82 440 (o)	7/2	0.10	1.51E+09	0.11	1.54E+09
2351.926	39 935 (e)	7/2	82 440 (o)	7/2	−0.43	4.48E+08	−0.42	4.57E+08
2352.085	40 071 (e)	7/2	82 573 (o)	5/2	−0.37	5.20E+08	−0.34	5.57E+08
2357.705	38 610 (e)	9/2	81 011 (o)	7/2	−0.63	2.81E+08	−0.62	2.89E+08
2359.469	40 071 (e)	7/2	82 440 (o)	7/2	0.07	1.40E+09	0.08	1.43E+09
2370.660	40 404 (e)	3/2	82 573 (o)	5/2	−0.71	2.35E+08	−0.68	2.52E+08
2433.728	39 935 (e)	7/2	81 011 (o)	7/2	−1.00	1.12E+08	−0.99	1.15E+08
2461.668	40 401 (e)	9/2	81 011 (o)	7/2	−0.65	2.47E+08	−0.64	2.54E+08
2474.414	36 406 (e)	7/2	76 807 (o)	9/2	−0.56	2.98E+08	−0.56	2.96E+08
2483.272	40 754 (e)	5/2	81 011 (o)	7/2	−1.02	1.03E+08	−1.01	1.06E+08
2499.418	36 810 (e)	5.5	76 807 (o)	9/2	−0.89	1.38E+08	−0.89	1.37E+08
2513.189	41 233 (e)	7/2	81 011 (o)	7/2	−0.75	1.86E+08	−0.74	1.91E+08
2534.751	37 368 (e)	7/2	76 807 (o)	9/2	−1.01	1.02E+08	−1.01	1.01E+08
2535.150	43 140 (e)	7/2	82 573 (o)	5/2	−0.46	3.64E+08	−0.43	3.90E+08
2536.167	43 022 (e)	9/2	82 440 (o)	7/2	−0.67	2.21E+08	−0.63	2.25E+08
2543.730	43 140 (e)	7/2	82 440 (o)	7/2	−0.66	2.27E+08	−0.65	2.32E+08
2576.239	43 768 (e)	5/2	82 573 (o)	5/2	−0.50	3.20E+08	−0.47	3.43E+08
2576.281	38 003 (e)	9/2	76 807 (o)	9/2	−0.82	1.51E+08	−0.82	1.50E+08
2585.101	43 768 (e)	5/2	82 440 (o)	7/2	−0.88	1.32E+08	−0.87	1.35E+08
2585.480	38 056 (e)	7/2	76 722 (o)	5/2	−0.83	1.47E+08	−0.78	1.64E+08
2593.518	38 175 (e)	3/2	76 722 (o)	5/2	−0.76	1.72E+08	−0.71	1.92E+08
2617.221	38 610 (e)	9/2	76 807 (o)	9/2	−0.26	5.39E+08	−0.26	5.35E+08
2624.136	42 915 (e)	5/2	81 011 (o)	7/2	−0.82	1.48E+08	−0.81	1.52E+08
2625.497	44 496 (e)	7/2	82 573 (o)	5/2	−0.88	1.28E+08	−0.85	1.37E+08
2631.544	43 022 (e)	9/2	81 011 (o)	7/2	−0.53	2.86E+08	−0.52	2.94E+08
2634.660	44 496 (e)	9/2	82 440 (o)	7/2	−0.16	6.70E+08	−0.15	6.83E+08
2634.701	44 496 (e)	7/2	82 440 (o)	7/2	−0.95	1.08E+08	−0.94	1.10E+08
2669.937	39 279 (e)	5/2	76 722 (o)	5/2	−0.66	2.04E+08	−0.61	2.27E+08
2687.146	39 604 (e)	5.5	76 807 (o)	9/2	−0.19	5.96E+08	−0.19	5.92E+08
2709.306	39 823 (e)	5/2	76 722 (o)	5/2	−0.36	3.94E+08	−0.31	4.39E+08
2727.637	40 071 (e)	7/2	76 722 (o)	5/2	0.13	1.22E+09	0.18	1.36E+09
2737.739	44 496 (e)	9/2	81 011 (o)	7/2	−0.95	1.01E+08	−0.64	1.04E+08
2838.714	45 795 (e)	7/2	81 011 (o)	7/2	−0.64	1.90E+08	−0.63	1.95E+08

[a] Wavelengths are deduced from the experimental energy levels. They are given in air above 2000 Å and in vacuum below that limit.
[b] From the NIST compilation (Martin *et al* 1978).
[c] HFR method including core-polarization corrections (see text).
[d] Normalized values using the experimental lifetimes reported in table 2.

effects on all orbitals produced by exciting an electron out of the deeply buried 4f subshell (see Cowan (1981)). The standard deviation, as defined by Cowan (1981), was reduced to 32 cm^{-1} for the odd parity (40 levels and 11 fitted parameters) and to 133 cm^{-1} for the even parity (80

levels and 17 fitted parameters).

Radiative lifetimes obtained for some $4f^{12}6p$ levels (calculation A) are reported in table 2, where they are compared with the experimental results. The agreement is good. As seen from table 2, for the $4f^{12}5d$ configuration, larger discrepancies are, however, observed for some levels when comparing theory to experiment. This is probably related to the crude approach which has been used for calculating matrix elements involving a 4f electron and which could lead to less accurate lifetime values, at least for some specific levels.

The effects of additional configurations of the type $4f^{11}nln'l'$, not included explicitly in our physical model A, were estimated in an additional separate semi-empirical HFR computation (calculation B). More precisely, the odd-parity configurations $4f^{11}5d^2$, $4f^{11}6s^2$ and $4f^{11}5d6s$ and the even-parity configurations $4f^{11}5d6p$ and $4f^{11}6s6p$ were investigated. For these configurations, the average energy level values were adjusted to reproduce the energies predicted by Brewer (1971) for the lowest level of each configuration, i.e. $4f^{11}5d^2\ {}^6L_{11/2}$ ($E = 85\,000 \pm 9000$ cm^{-1}), $4f^{11}6s^2\ {}^4I_{15/2}$ ($E = 115\,000 \pm 7000$ cm^{-1}), $4f^{11}5d6s\ {}^6K_{13/2}$ ($E = 100\,000 \pm 5000$ cm^{-1}), $4f^{11}5d6p\ {}^6L_{11/2}$ ($E = 136\,000 \pm 7000$ cm^{-1}) and $4f^{11}6s6p\ {}^6I_{15/2}$ ($E = 150\,000 \pm 9000$ cm^{-1}).

It has appeared that the theoretical lifetimes obtained using the approach B and not reported in table 2 were 15–20% longer than the experimental results. This is related to the fact that the effects of the $4f^{11}nln'l'$ configurations are already taken into account in the core-polarization corrections included in the calculations so that simultaneous consideration of these corrections and explicit introduction of $4f^{11}nln'l'$ configurations lead to an overestimation of the core-polarization effects.

A selected sample of HFR (calculation A) oscillator strengths and transition probabilities for Tm III lines is presented in table 3. In addition to the HFR data, we give also in the table normalized results deduced from the experimental lifetimes reported in this paper and theoretical branching fractions. The complete table is available in our DREAM (Database on Rare-Earths at Mons University) atomic database at the address http://www.umh.ac.be/∼astro/dream.shtml. For most of the transitions, particularly for the most intense ones, these results are expected to be accurate within a few per cent. The uncertainties could, however, be larger when a 4f electron is involved in the transitions. Additional lifetime measurements for a larger number of levels would be welcome to verify this assumption.

Acknowledgments

This work was partly supported by the European Community Access to Large-Scale Facilities programme (contract ERBFMGECT 950020). Financial support from the Swedish Natural Science Research Council (NFR) and from the Belgian National Fund for Scientific Research (FNRS) is also gratefully acknowledged. Some of us (TB, EB, HPG, PQ) have highly appreciated the warm hospitality of the Lund Laser Centre and would like to thank all the members of the LLC team for their kindness and efficiency.

References

Anderson H M, Den Hartog E A and Lawler J E 1996 *J. Opt. Soc. Am.* B **13** 2382

Biémont E, Dutrieux J-F, Martin I and Quinet P 1998 *J. Phys. B: At. Mol. Opt. Phys.* **31** 3321

Biémont E, Li Z S, Palmeri P and Quinet P 1999 *J. Phys. B: At. Mol. Opt. Phys.* **32** 3409

Biémont E, Garnir H P, Bastin T, Palmeri P, Quinet P, Li Z S, Zhang Z G, Lokhnygin V and Svanberg S 2001 *Mon. Not. R. Astron. Soc.* **321** 481

Bord D J, Cowley C R and Norquist P L 1997 *Mon. Not. R. Astron. Soc.* **284** 869
Brewer L 1971 *J. Opt. Soc. Am.* **61** 1666
Cowan R D 1981 *The Theory of Atomic Structure and Spectra* (Berkeley, CA: University of California press)
Cowley C R and Bord J 1998 *Astron. Soc. Pac. Conf. Ser.* **143** 346
Fedchak J A, Den Hartog E A, Lawler J E, Palmeri P, Quinet P and Biémont E 2000 *Astrophys. J.* **542** 1109
Fraga S, Karwowski J and Saxena K M S 1976 *Handbook of Atomic Data* (Amsterdam: Elsevier)
Li Z S and Jiang Z 1999 *Phys. Scr.* **60** 414
Li Z S, Lundberg H, Wahlgren G M and Sikström C M 2000 *Phys. Rev.* A **62** 032505
Li Z S, Norin J, Persson A, Wahlström C-G, Svanberg S, Doidge P S and Biémont E 1999b *Phys. Rev.* A **60** 198
Li Z S, Svanberg S, Quinet P, Tordoir X and Biémont E 1999a *J. Phys. B: At. Mol. Opt. Phys.* **32** 1731
Martin W C, Zalubas R and Hagan L 1978 *Atomic Energy Levels—The Rare Earth Elements* NBS 60 (Washington, DC: US Govt Printing Office)
Quinet P, Palmeri P and Biémont E 1999a *J. Quant. Spectrosc. Radiat. Transfer* **62** 625
Quinet P, Palmeri P, Biémont E, McCurdy M M, Rieger G, Pinnington E H, Wickliffe M E and Lawler J E 1999b *Mon. Not. R. Astron. Soc.* **307** 934
Spector N, Sugar J and Wyart J-F 1997 *J. Opt. Soc. Am.* B **14** 511
Sugar J 1970 *J. Opt. Soc. Am.* **60** 454
Wahlgren G M *et al* 2001 in manuscript
Wyart J F, Blaise J, Bidelman W P and Cowley C R 1997 *Phys. Scr.* **56** 446
Wyart J F, Blaise J and Camus P 1974 *Phys. Scr.* **9** 325
Wyart J F and Palmeri P 1998 *Phys. Scr.* **58** 368
Zhang Zhiguo, Li Z S, Lundberg H, Zhang K Y, Dai Z W, Jiang Zhankui and Svanberg S 2000 *J. Phys. B: At. Mol. Opt. Phys.* **33** 521